JOURNAL OF MATERIALS SCIENCE **40** (2005) 1087–1091

Metal-nonmetal transition and the electronic transport behavior in disordered PbO_2-Ag_2O-xC system synthesized by ball milling

D. LI, D. Y. GENG, Y. T. XING, W. F. LI, G. W. QIAO, Y. Z. WANG, Z. D. ZHANG
Shenyang National Laboratory for Materials Science, Institute of Metal Research, and International Centre for Materials Physics, Chinese Academy of Sciences, Shenyang 110016, People's Republic of China

The electronic transport properties as a function of temperature and the graphite content have been investigated for disordered PbO_2-Ag_2O-xC ($0 \leq x \leq 3$) composite materials. The components of the system change from (1) lead-silver oxides of $Ag_5Pb_{2.5}O_6$ and/or Ag_2PbO_2 to (2) $PbCO_3$ + $2PbCO_3{\cdot}PbO$ + Ag and (3) $PbCO_3$ + Ag + Pb with increasing the graphite content. $Ag_5Pb_2O_6$ is synthesized directly by mechanical milling with a simple solid-state reaction of Ag_2O and PbO_2. The structure, thermal and electric properties of silver-lead oxides are characterized by means of X-ray diffraction, scanning electron microscope, a differential scanning calorimeter analysis and DC resistivity measurements. Strengthening the degree of disorder through mechanical milling and/or doping the lead oxide into $Ag_5Pb_2O_6$ causes the conductivity transition from metallic to semiconducting behavior, while decreasing the degree of disorder by annealing and the segregation of the lead oxide from the solid solution leads to a reverse transition.

1. Introduction

Metal-nonmetal transition has been an interesting topic in the field of condensed matter physics. It is very important to find new metal-nonmetal transitions and understand the mechanisms of the metal-nonmetal transitions in various materials. Recently, possible occurrence of a superconductor in the $PbCO_3{\cdot}2PbO$-Ag_2O and $PbCO_3{\cdot}PbO$-Ag_2O systems was revealed by Djurek *et al*. [1, 2]. According to their report, the compounds of $PbCO_3{\cdot}PbO$ and $PbCO_3{\cdot}2PbO$ with layer structure doped by Ag_2O (Ag_2CO_3) may result in a number of novel metals. An Ag-Pb-C-O compound with behaviors showing the possibility of superconducting, which had a main X-ray diffraction peak of $d = 3.21$ Å, was prepared by solid-state reactions at high pressure in $O_2 + CO_2$ atmosphere [1, 2]. The impurity phase in Ag-Pb-C-O compound [1, 2] was found to be concerned with $Ag_5Pb_2O_6$. The formation and characterization of $Ag_5Pb_2O_6$ were investigated further by several methods [3–5]. More recently, we investigated the structures and the electronic transport properties of PbO_2-$\frac{1}{12}Ag_2O$-xC system and PbO_2-$x\,Ag_2O$-0.75C system, which showed that abundant phase transformations and percolation effect exist with increasing graphite or Ag_2O contents [6, 7]. By means of DC resistivity and X-ray diffraction (XRD) measurements, we confirmed the percolation thresholds $x_c = 0.75$ in the PbO_2-$\frac{1}{12}Ag_2O$-xC system [6] and $x_c = 0.275$ in the PbO_2-$x\,Ag_2O$-0.75C system [7], respectively.

$Ag_5Pb_2O_6$ compound was firstly prepared by hydrothermal synthesis method [8] in trigonal form (space group $P31m$). Jansen and coworkers reported the hexagonal structure through high-pressure synthesis method [9]. In the present work, by mechanical milling at room temperature under ambient pressure, we study the electronic transport behavior and examine the effect of graphite on the resistivity of a disordered PbO_2-Ag_2O system and also report the synthesis, thermal behavior, and electric properties of $Ag_5Pb_2O_6$. As the mixture of PbO_2, Ag_2O and graphite is milled, nanocomposited PbO_2-Ag_2O-xC materials show some interesting phenomena on electronic transport properties, such as metal-nonmetal transition [10], depending on the compositions/disorder of the system.

2. Experimental details

Reagent grade PbO_2 (rutile-type), Ag_2O and 99.7%-pure graphite obtained by milling graphite flakes for 5h were employed as the starting materials. PbO_2 is a white colored substance, which commonly turns into black or brown as containing trances of water and/or OH^- groups [11]. The presence of the water and/or carbonates was estimated by the use of the Perkin-Elmer infrared spectrometer and absorption spectra of PbO_2 and Ag_2O powders mixed with KBr. For PbO_2 powders, OH stretching absorption band is positioned at 3445 cm^{-1} and H_2O bending absorption band at 1635 cm^{-1}. The

latter should be compared to the bending absorption band at 1595 cm^{-1} of H_2O vapor. The absorption band analysis excluded the possibility of CO_3 absorption band coming from the traces of lead carbonate in our starting material of PbO_2. Infrared absorption spectrum at the absorption bands of 3450 cm^{-1} and 1653 cm^{-1} indicated that the trances of water exist in the starting material of Ag_2O, while absorption band at 1418 cm^{-1} in the IR spectrum of Ag_2O showed that a small amount of Ag_2CO_3 accompanies Ag_2O powders.

The nanocomposite materials of PbO_2-Ag_2O-xC system were prepared from PbO_2, Ag_2O and C with the molar ratio of 1:1:x ($0 \leq x \leq 3$). $Ag_5Pb_2O_6$ was prepared with the molar ratio of PbO_2: $Ag_2O = 2{:}2.5$. The powder mixtures of the starting materials were sealed in a hardened steel can in an air atmosphere and mechanically milled using a high-energy ball mill with rotational speed of 800 rpm for 5 h. The mass ratio of ball to powder was 20:1.

XRD patterns were recorded at room temperature using Cu K_α radiation with a Rigaku D/Max 2500 PC rotation target diffractometer. The power of the XRD diffractometer was adjusted to 50 kV and 250 mA during the analysis. Morphology of the particles was examined by a scanning electron microscope (SEM; XL30, PHILIPS). The quantitative analyses were performed by the induction coupled plasma (ICP) spectroscopy for Ag and Pb in the $Ag_5Pb_2O_6$ sample. The as-milled powders were pressed into pellets by using a 700 MPa axial-pressure with a steel die. The pellets were ground to a rectangular parallelepiped with dimensions of $1.5 \times 6 \times 0.6\,mm^3$ to fit the test holder. The temperature dependence of electric resistivity was measured using superconducting quantum interference device (SQUID, Quantum Design) by the DC four-probe method with contact resistance smaller than 1 Ω. The differential scanning calorimeter (DSC) analysis was performed on the desired powder samples in the flow of Argon at the heating rate of 20 K/min using Perkin-Elmer DSC-7.

3. Results and discussion

After milled for 5 h, the dark or brown powders were produced. When the cans were opened, some gases ejected from the cans. When the gases were collected, a part of the gases can be absorbed by a solution of ~20% NaOH, which was considered as CO_2. The gases produced during milling consist of O_2 and/or CO_2, depending on the content of graphite in the precursors. Furthermore, the amount of the gases increases with increasing the content of graphite. The pellets pressed show metallic luster. XRD patterns (Fig. 1) show a sequential transformation of the phase constituents of the as-milled powders with different graphite contents and none of the unreacted PbO_2 exists. It is clear that some solid-state reactions between the oxidants of PbO_2, Ag_2O and the reductant of graphite occur indeed during milling through strenuous impacts. The XRD patterns of the samples without or with a small amount of graphite ($0 \leq x \leq 0.3$) show broad peaks of a solid solution of $Ag_5Pb_2O_6$ doped by lead oxide. The possible reaction is: $5Ag_2O + 4PbO_2 \rightarrow 2Ag_5Pb_2O_6 + 1/2O_2$. With increasing the graphite content, the solid reactions between Ag_2O, PbO_2 and graphite happen together. The phase $Ag_5Pb_2O_6$ gradually transforms to Ag_2PbO_2, $PbCO_3$, $2PbCO_3{\cdot}PbO$ and Ag for $x = 0.5$ and 0.75, and the reactions are a little complex. For $x = 1$ and 1.25, the systems mainly consist of the mixture of $PbCO_3$ and Ag. From $x = 1.5$ to $x = 3$, similar to the sample of $x = 2$ as shown in Fig. 1, the amount of $PbCO_3$ gradually decreases and some Pb and PbO emerge for the reduction of graphite and oxidation of lead.

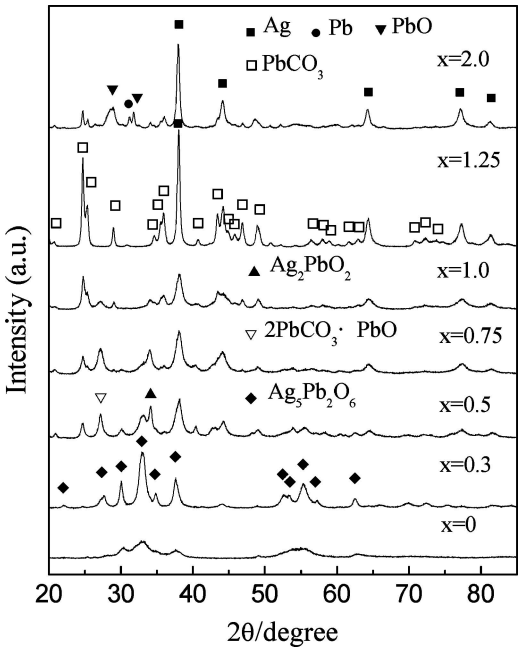

Figure 1 X-ray diffraction patterns of the as-milled PbO_2-Ag_2O-xC samples.

The temperature dependences of electric resistivity of the pellets prepared by pressing the as-milled powders are shown in Fig. 2. The resistivity of the sample $x = 0.1$ increases with decreasing temperature, which exhibits negative temperature coefficient of resistivity with semiconducting behavior. The conductivity of the samples changes from semiconductivity ($x = 0.1$) to metallic behavior ($x \geq 0.25$), which is ascribed to a metal-nonmetal transition [10, 12, 13], due to the extent of disorder. Disorder induced by defects and insulating phase during the mechanical milling process is expected to reduce the electric mean free path and thus the electric conductivity. When the mean free path becomes less than the inter-atomic spacing, a coherent metallic transport would not be possible. With a change of the phase constituents in the PbO_2-Ag_2O-xC systems, the component, the relative amount and the distribution of the conductive phase have been changed. As $x \leq 0.3$, the phase of $Ag_5Pb_2O_6$ shows the conductivity. For the samples of $x = 0.5$ and 0.75, the conductive components, such as $Ag_5Pb_2O_6$ and Ag particles, are included. When $0.2 \leq x \leq 0.75$, the temperature coefficient of resistivity changes from positive to negative with cooling. The arrow below the curves marks the resistivity minimum $\rho_{\min}$. The anomalous, negative temperature coefficient of resistivity exhibits below the temperature for ρ_{min}, depending on the elastic mean free path of

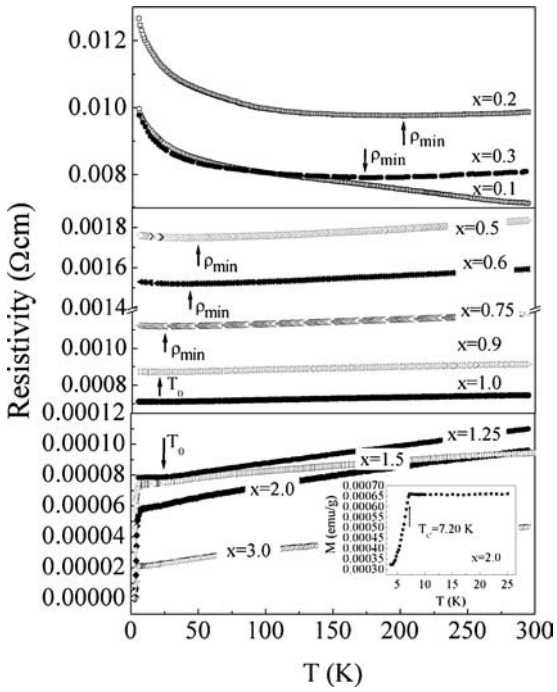

Figure 2 Temperature dependence of resistivity of the as-milled PbO_2-Ag_2O-xC samples. The inset shows the temperature dependence of DC susceptibility of the sample with $x = 2$ at an applied field of 20 Oe.

free carriers, similar to that described in the literatures [14, 15]. In fact, such a behavior was predicted in the interpretation of the origin of the Mooij correlation [16]. The samples of $0.9 \leq x \leq 1.25$, consisting of Ag particles as the conductive components, show metallic conductivity, which are characterized by a linear function of $\rho = \rho_0 + AT$ (where ρ is resistivity of the composite, ρ_0 residual resistivity due to impurity scattering ($T < T_0$) and A the temperature coefficient of resistivity) in the measurement temperature range. It can be illustrated by the scattering of conduction electron by thermal vibration of atoms. However, the samples for $1.5 \leq x \leq 3.0$, which are composed of finely dispersed Ag and Pb as the conductive components, exhibit superconducting transitions near to 7.20 K. DC magnetic susceptibility measurement at an applied field of 20 Oe (shown as the inset of Fig. 2) confirms that the superconductivity is caused by Pb particles in these samples. It indicates that Pb particles reduced by graphite engage in electric conduction, which form a conductive path through the insulating matrix of $PbCO_3$ and PbO, so that the concentrations of Pb particles are higher than the percolation threshold (x_{Pb}).

Scanning electron micrograph (SEM) of the $Ag_5Pb_2O_6$ sample annealed at 673 K in 0.1 MPa O_2 flow for 30 min is shown in Fig. 3, which indicates that the particle size of the powders is in the order of nanometers. The particles, shown in Fig. 3, are analyzed by energy-dispersive X-ray technique (Fig. 4), which gives qualitative indication of the Ag and Pb elements in these particles. Copper and carbon elements detected in Fig. 4 come from the copper grid, which is coated with carbon film used to mount the powder specimens. Quantitative chemical analysis by the induction coupled plasma (ICP) spectroscopy for Ag and Pb in $Ag_5Pb_2O_6$ sample shows the molar ratio

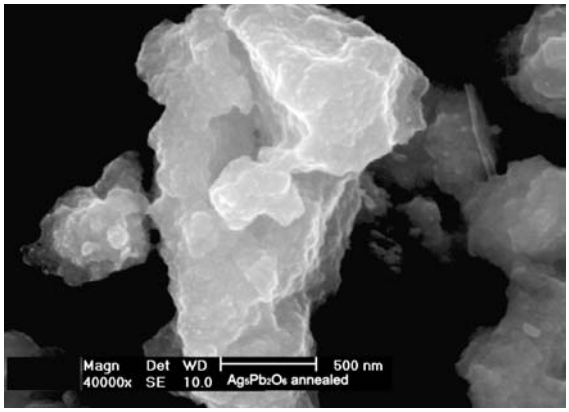

Figure 3 Scanning electron micrograph (SEM) of $Ag_5Pb_2O_6$ sample annealed at 673 K in the flow of oxygen at 0.1 MPa.

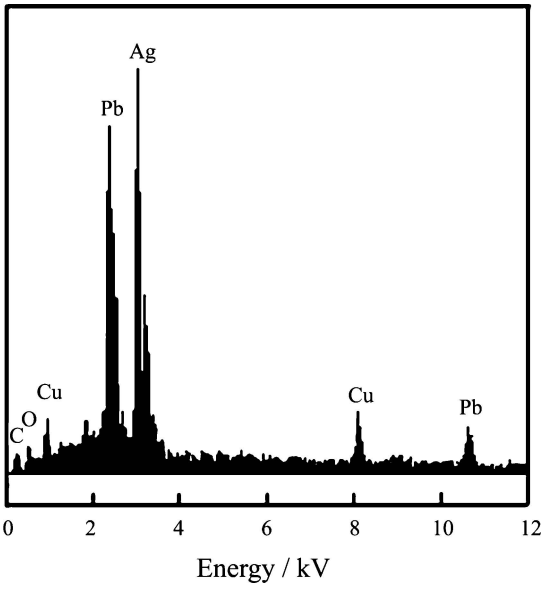

Figure 4 Energy-dispersive X-ray analysis (EDX) pattern of the particles shown in Fig. 3.

"[Ag]/[Pb]" to be 2.49 in the agglomerated particles, in good agreement with the nominal composition of the starting mixture. The extent of iron traces in the final products analyzed by ICP is about 0.1% by weight, thus the iron element cannot be indicated in Fig. 4.

Fig. 5 shows the DSC curves of (a) $x = 0$ and (b) $Ag_5Pb_2O_6$ samples performed on heating process. The endothermal peaks below 400 K are caused by the release of the gas and the trances of water absorbed, because of the large specific surface area of the as-milled powder samples. The DSC curve of the as-milled $Ag_5Pb_2O_6$ sample (Fig. 5b) reveals that three endothermal transitions occur with the peak temperatures at 791, 825 and 848 K, respectively. Fig. 6 exhibits the XRD patterns of (a) the as-milled $Ag_5Pb_2O_6$ and (b) that annealed at 673 K in 0.1 MPa O_2 flow for 30 min, which indicate that hexagonal $Ag_5Pb_2O_6$ can be synthesized by mechanical milling method with sequential annealing process below the decomposition temperature of $Ag_5Pb_2O_6$. The crystal structure of $Ag_5Pb_2O_6$ as shown in Fig. 6b is same as that reported by Jansen and coworkers [9]. We try to identify these transitions occurred in Fig. 6b by annealing the as-milled $Ag_5Pb_2O_6$ at

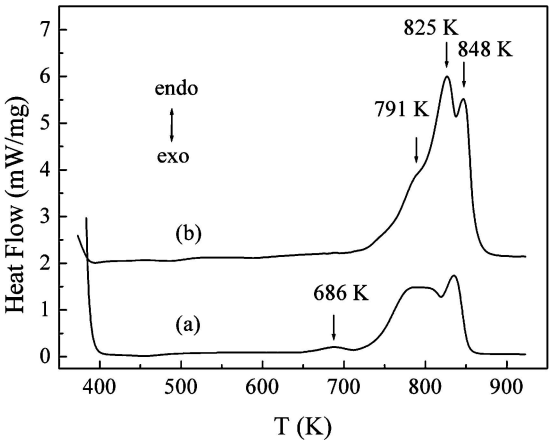

Figure 5 DSC curves of (a) $Ag_5Pb_{2.5}O_6$ ($x = 0$) and (b) $Ag_5Pb_2O_6$ samples performed on heating process.

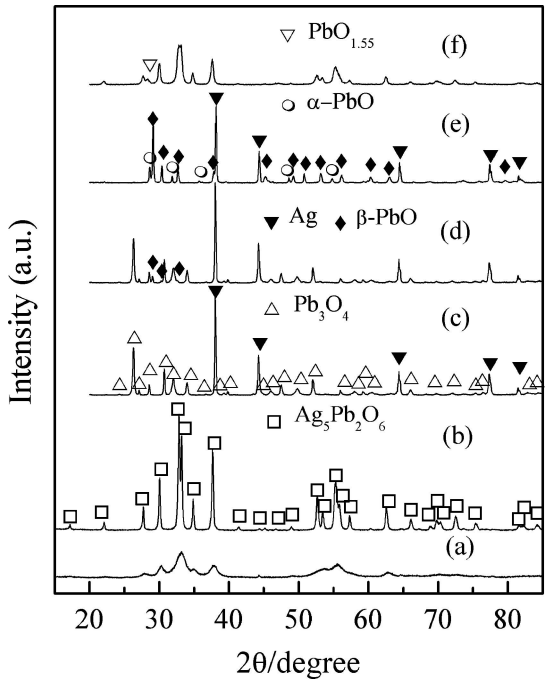

Figure 6 X-ray diffraction patterns of (a) the as-milled $Ag_5Pb_2O_6$, (b) $Ag_5Pb_2O_6$ annealed at 673 K in the flow of O_2, and the samples of $Ag_5Pb_2O_6$ annealed at (c) 783 K, (d) 813 K, (e) 873 K in air atmosphere, respectively, (f) the $Ag_5Pb_{2.5}O_6$ annealed at 663 K in vacuum.

different temperatures of 783, 813 and 873 K, respectively, in an air atmosphere. After quench from 783 K, XRD pattern (Fig. 6c) confirms that $Ag_5Pb_2O_6$ is decomposed to Ag, Pb_3O_4 and O_2 as follows:

$$3Ag_5Pb_2O_6 \rightarrow 15Ag + 2Pb_3O_4 + 5O_2 \uparrow \quad (1)$$

The formation of PbO is confirmed by XRD pattern (Fig. 6d) of the sample obtained after heating at 813 K, following the decomposition reaction:

$$Pb_3O_4 \rightarrow 3PbO + \frac{1}{2}O_2 \uparrow \quad (2)$$

Both of the decompositions as shown as reactions (1) and (2) above are consistent with those reported for $Ag_5Pb_2O_6$ [3, 8]. However, we find a crystal structure transition from β-PbO to α-PbO (Fig. 6e) during a heating process of $Ag_5Pb_2O_6$ with a peak temperature of 848 K as shown in Fig. 5b. The different preparation process of $Ag_5Pb_2O_6$ sample may influence its thermal property and lead to the additional structure transition of PbO. Compared with the DSC curve in Fig. 5b, except for the same three endothermal peaks at 791, 825 and 848 K, respectively, there is more than one endothermal peak with an peak temperature of 686 K appearing in Fig. 5a, which corresponds to the segregation of $PbO_{1.55}$ from the solid solution of $Ag_5Pb_{2.5}O_6$ ($x = 0$) after annealed at 663 K in 2×10^{-3} Pa for 30 min. as described in Fig. 6f. In addition, $PbCO_3$·PbO-Ag could be obtained by annealing the sample of $x = 1.0$ at 523 K in air. Because it is difficult to reach the exactly same condition as that in literatures [1, 2], we could not have synthesized the phase 321.

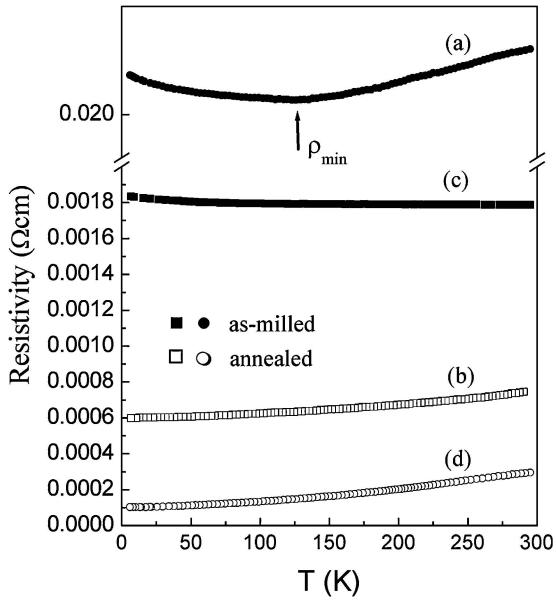

Figure 7 Temperature dependence of resistivity of the samples for (a) the as-milled $Ag_5Pb_2O_6$, (b) $Ag_5Pb_2O_6$ annealed at 673 K in the flow of O_2, (c) the as-milled $Ag_5Pb_{2.5}O_6$, (d) $Ag_5Pb_{2.5}O_6$ annealed at 663 K in vacuum.

Fig. 7 exhibits the temperature dependence of electric resisitivity of the samples for (a), (b) $Ag_5Pb_2O_6$ and (c), (d) $Ag_5Pb_{2.5}O_6$. It is noticed that the mechanical milling process could introduce the disorder into the system. The effect consequently changes the electric conductivity of the material. A transition from metallic conductivity to semiconductivity occurs in the as-milled $Ag_5Pb_2O_6$ (Fig. 7a). Furthermore, the effect of non-stoichiometry increases the degree of disorder by doping the lead oxide into the $Ag_5Pb_2O_6$. As a result of the enhancement of disorder, the as-milled sample $Ag_5Pb_{2.5}O_6$ exhibits semiconductivity in the temperature range from 5 to 295 K as shown in Fig. 7c. The previous work [17] showed transformation of conductivity behavior of $Ag_5Pb_2O_6$ for partial substitution of Pb^{4+} by other cations, Bi^{3+} and In^{3+}. The series $Ag_5Pb_{2-x}M_xO_6$ ($0 \leq x \leq 1$ for M = Bi, and $0 \leq x \leq 0.75$ for M = In) were synthesized at temperature close to 800°C under high O_2 pressures of 100 MPa for 4 days [17]. Replacement of a small fraction of Bi^{3+} for Pb^{4+} resulted in a drastic increase in resistivity and a transition of conductivity of $Ag_5Pb_{2-x}Bi_xO_6$ from metallic

behavior ($x = 0$) to semiconducting behavior ($0.25 \leq x \leq 0.75$) and insulator ($x = 1$). In the series of the solid solution $Ag_5Pb_{2-x}Cu_xO_6$ ($0 \leq x \leq 0.5$) [18], the substitution of copper for lead results in a drastic change of electric resistivity, similar to what was found for the family $Ag_5Pb_{2-x}Bi_xO_6$ [17]. As mentioned above, the mechanical milling process and doping the lead oxide into $Ag_5Pb_2O_6$ introduce the disorder into the systems, changing the electric transport properties of $Ag_5Pb_2O_6$. After annealed, $Ag_5Pb_2O_6$ and $Ag_5Pb_{2.5}O_6$ ($x = 0$) show the metallic conductive behavior (Fig. 7b and d), which should be due to the thermal activation leading to the transformation of disorder to order.

4. Conclusions

In this paper, a new alternative method to directly synthesize hexagonal $Ag_5Pb_2O_6$ is developed by mechanical milling with a simple solid-state reaction of Ag_2O and PbO_2. The effects of graphite on conductivity of the nanocomposite disordered PbO_2-Ag_2O-xC materials prepared by mechanical milling have been investigated. With increasing the graphite content, the components of the system change from (1) lead-silver oxides of $Ag_5Pb_{2.5}O_6$ and/or Ag_2PbO_2 to (2) $PbCO_3$ + $2PbCO_3{\cdot}PbO$ + Ag and (3) $PbCO_3$ + Ag + Pb, and the conductivity of the PbO_2-Ag_2O-xC system undergoes a metal-nonmetal transition. With strengthening the degree of disorder through mechanical milling and/or doping the lead oxide into $Ag_5Pb_2O_6$, the conductivity of silver-lead oxide experiences a transition from metallic to semiconducting behavior, while decreasing the degree of disorder by annealing and the segregation of the lead oxide from the solid solution leads to a reverse transition.

Acknowledgment

This work has been supported by the National Nature Science Foundation of China (Grant Number 50332020 and 59725103) and the Science and Technology Commissions of Shenyang. Zhang thanks the helpful discussion of Prof. G H Wu.

References

1. D JUREK, Z. MEDUNIĆ, A. TONEJC and M. PALJEVIĆ, *Physica C* **341–348** (2000) 723.
2. *Idem. ibid.* **351** (2001) 78.
3. K. IWASAKI, H. YAMANE, S. KUBOTA, J. TAKAHASHI, Y. MIYAZAKI, T. KAJITANI, K. NAKAJIMA,T. TAMASHITA and M. SHIMADA, *ibid.* **382** (2002) 263.
4. H. ABE, J. H. YE, M. IMAI, K. YOSHII, A. MATSUSHITA and H. KITAZAWA, *J. Cryst. Growth* **241** (2002) 347.
5. L. T. DING, C. J. ZHANG, Y. H. ZHANG and H. H WEN, *Physica C* **399** (2003) 178.
6. D. LI, Z. D. ZHANG, D. Y. GENG, W. F. LI, X. P. SONG, G. W. QIAO and Y. Z. WANG, *Solid State Commun.* **125** (2003) 493.
7. W. F. LI, Z. D. ZHANG, D. LI and X. G. ZHAO, *J. Phys. D.: Appl. Phys.* **37** (2004) 1853.
8. A. BYSTRÖM and L. EVERS, *Acta Chem. Scand.* **4** (1950) 613.
9. M. JANSEN, M. BORTZ and K. HEIDEBRECHT, *J. Less-Common Met.* **161** (1990) 17.
10. A. F. IOFFE and A. R. REGEL, *Prog. Semicond.* **4** (1960) 237.
11. H. HARADA, Y. SASA and M. UDA, *J. Appl. Crystallogr.* **14** (1981) 1441.
12. N. F. MOTT and E. A. DAVIS, in "Electronic Processes in Noncrystalline Materials" (Oxford University Press, Oxford, 1979) Chap. 4.
13. N. F. MOTT, "Metal-Insulator Transition," (Taylor & Francis, London, 1990).
14. I. SCHWARTZ, S. SHAFT, A. MOALEM and Z. OVADYHU, *Phil. Mag. B* **50** (1984) 221.
15. J. H. MOOIJ, *Phys. Status Solidi A* **17** (1973) 521.
16. M. KAVEH and N. F. MOTT, *J. Phys. C: Solid State Phys.* **15** (1982) L707.
17. M. BORTZ, M. JANSEN, H. HOHL and K. BUCHER, *J. Solid State Chem.* **103** (1993) 447.
18. E. M. TEJADA-ROSALES, J. OR-SOLE and P. GMEZ-ROMERO, *ibid.* **163** (2002) 151.

Received 28 September
and accepted 22 November 2004